Cyclometallation Following Coordination of Anionic and Neutral Lewis Bases to a Uranium(IV) Dialkyl Complex

Nicholas R. Andreychuk,[†] *David J. H. Emslie,*[*,†] *Hilary. A. Jenkins,*[‡] *and James F. Britten*[‡]

† Department of Chemistry, McMaster University, 1280 Main Street West, Hamilton, Ontario, L8S 4M1, Canada. Fax: (905)-522-2509; Tel: (905)-525-9140 x 23307.

E-mail: emslied@mcmaster.ca. Website: http://www.chemistry.mcmaster.ca/emslie/emslie.html

‡ McMaster Analytical X-Ray Diffraction Facility, 1280 Main Street West, Hamilton, Ontario, L8S 4M1, Canada

ABSTRACT

Addition of 3.05 equiv of dme (1,2-dimethoxyethane) to an *n*-pentane solution of [(XA_2)U(CH_2SiMe_3)$_2$] (**1**; XA_2 = 4,5-bis(2,6-diisopropylanilido)-2,7-di-*tert*-butyl-9,9-dimethylxanthene) and $LiCH_2SiMe_3$ (~1:1) precipitated the tris(alkyl) 'ate' complex, [Li(dme)$_3$][(XA_2)U(CH_2SiMe_3)$_3$] (**2-dme**). Sterically encumbered **2-dme** is thermally unstable in solution, eliminating $SiMe_4$ to form [Li(dme)$_3$][(XA_2*)U(CH_2SiMe_3)$_2$] (**3-dme**; XA_2* = XA_2 cyclometallated at the methine carbon of an isopropyl group) as the major product. Compound **1** did not react with PMe_3, 2,2′-bipyridine (bipy), or quinuclidine in benzene at 40 °C. However, **1** reacted with 2.1 equiv of 4-(dimethylamino)pyridine (DMAP) or 9-azajulolidine (AJ; a DMAP derivative featuring a fused tricyclic structure) at 25 °C to afford [(XA_2)U(CH_2SiMe_3)(η^2*CN*-DMAP*)(DMAP)] (**4**) and [(XA_2)U(CH_2SiMe_3)(η^2*CN*-AJ*)(AJ)] (**5**), respectively, where DMAP* and AJ* are DMAP and AJ ligands cyclometallated at the 2-position. Reaction of **1** with DMAP-d_2 (deuterated in the *ortho* positions) confirmed that **4** is formed *via* a direct σ-bond metathesis mechanism. All newly-isolated uranium complexes (**2**–**5**) were crystallographically characterized.

Introduction

Multidentate non-carbocyclic ancillary ligands provide enormous opportunity to tune the steric, electronic and geometric environment at coordinated metal centres, providing a mechanism to influence and control a broad range of properties, including thermal stability and catalytic activity. One program of research in the Emslie group involves the application of highly-rigid pincer ligands to the development of thermally-robust organo-f-element complexes, and we previously reported the synthesis of a range of f-element complexes bearing 4,5-bis(anilido)xanthene dianions (these xanthene-backbone ligands are rigid in the sense that they ensure tridentate coordination, and strongly encourage meridional coordination, although the ligand backbone can bend to a significant degree, especially upon coordination to smaller metals [1, 2] or upon cyclometallation; *vide infra*). These complexes include neutral dialkyl thorium [3] and uranium [4] species, cationic monoalkyl thorium complexes [5, 6], neutral monoalkyl yttrium [2] and lutetium [7] complexes, and an anionic dialkyl complex of lanthanum [7] (Figure 1).

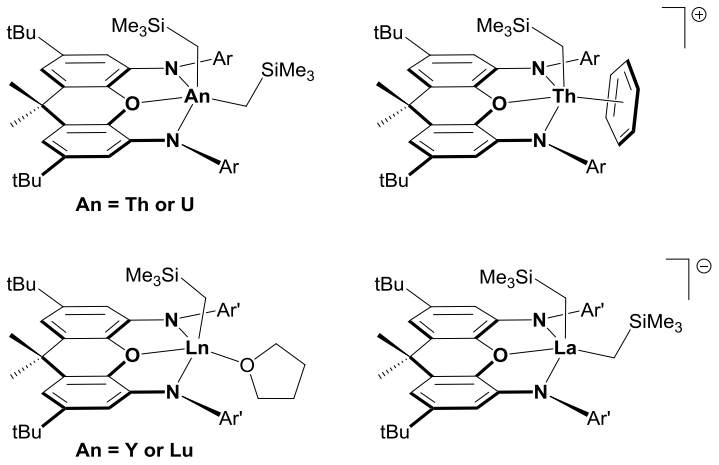

Figure 1. Selected 4,5-bis(anilido)xanthene f-element alkyl complexes (Ar = $C_6H_3{}^iPr_2$-2,6; Ar' = $C_6H_2{}^iPr_3$-2,4,6).

During the course of our investigations into the organometallic chemistry of uranium(IV), we uncovered the unusual reaction of $[(XA_2)U(CH_2SiMe_3)_2]$ (**1**; XA_2 = 4,5-bis(2,6-diisopropylanilido)-2,7-di-*tert*-

butyl-9,9-dimethylxanthene) with 2 equiv of $LiCH_2CMe_3$ in C_6D_6 to form the bis(neopentyl) complex $[(XA_2)U(CH_2CMe_3)_2]$, with release of 2 equiv of $LiCH_2SiMe_3$ (Scheme 1). This reaction resembles salt metathesis, but with elimination of a lithium alkyl rather than a lithium halide, and presumably proceeds via $[(XA_2)U(CH_2SiMe_3)_2(CH_2CMe_3)]^-$. However, no tris(alkyl) 'ate' complex could be detected in the reaction, or upon treatment of **1** with 20 equiv of $LiCH_2SiMe_3$ in C_6D_6 (Scheme 1). By contrast, neutral **1** reacted readily with $LiCH_2SiMe_3$ in THF-d_8 to afford $[Li(THF)_x][(XA_2)U(CH_2SiMe_3)_3]$ (**2-THF**), which was characterized *in-situ* by ^{1}H NMR spectroscopy [4].

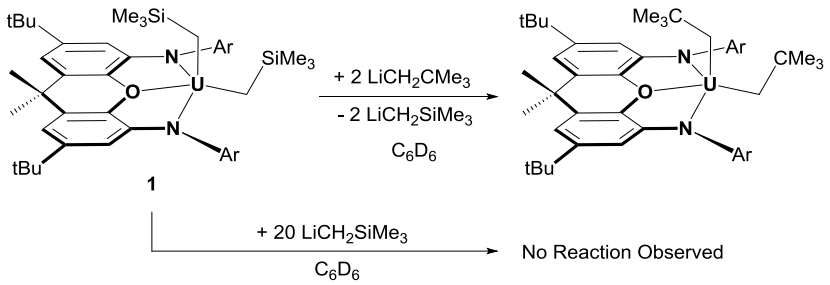

Scheme 1. Treatment of $[(XA_2)U(CH_2SiMe_3)_2]$ (**1**) in C_6D_6 with (a) 2 equiv of $LiCH_2CMe_3$ to afford $[(XA_2)U(CH_2CMe_3)_2]$, and (b) 20 equiv of $LiCH_2SiMe_3$ (Ar = $C_6H_3{}^iPr_2$-2,6).

Herein we report the isolation and structural characterization of $[Li(dme)_3][(XA_2)U(CH_2SiMe_3)_3]$ (**2-dme**) and its thermal decomposition product, in which a 2,6-diisopropylphenyl group is cyclometallated at the isopropyl methine position. Additionally, we describe the ability of pyridine Lewis bases to coordinate and subsequently engage in cyclometallation upon reaction with $[(XA_2)U(CH_2SiMe_3)_2]$ (**1**).

Results and Discussion

Reaction of $[(XA_2)U(CH_2SiMe_3)_2]$ (1) with $LiCH_2SiMe_3$: As noted above, $[Li(THF)_x][(XA_2)U(CH_2SiMe_3)_3]$ (**2-THF**) could be generated via the reaction of $[(XA_2)U(CH_2SiMe_3)_2]$ (**1**) with 1 equiv of $LiCH_2SiMe_3$ in THF [4]. However, **2-THF** is unstable in solution at room temperature; decomposition is noticeable in the ^{1}H NMR spectrum after 1 hour, and proceeds to

completion over the course of 1 week, accompanied by a solution colour change from yellow to dark-amber. Given the instability of **2-THF** in solution, previous attempts to isolate pure samples of **2-THF** were unsuccessful. The synthesis of **2** was also conducted in dme (1,2-dimethoxyethane) rather than THF, in the hope of improving product crystallinity, and while this approach afforded single crystals of $[Li(dme)_3][(XA_2)U(CH_2SiMe_3)_3]\cdot 2$ dme (**2-dme**·2 dme; *vide infra*), bulk material generated by this method was impure. Analytically pure **2-dme** was ultimately prepared by cooling an *n*-pentane solution of $[(XA_2)U(CH_2SiMe_3)_2]$ (**1**) and $LiCH_2SiMe_3$ (approx 1:1 stoichiometry) to −30 °C, followed by addition of 3.05 equiv of dme, resulting in rapid precipitation of **2-dme** as a yellow powder in 95% yield (Scheme 2).

Scheme 2. Synthesis of $[Li(dme)_3][(XA_2)U(CH_2SiMe_3)_3]$ (**2-dme**) (Ar = $C_6H_3{}^iPr_2$-2,6).

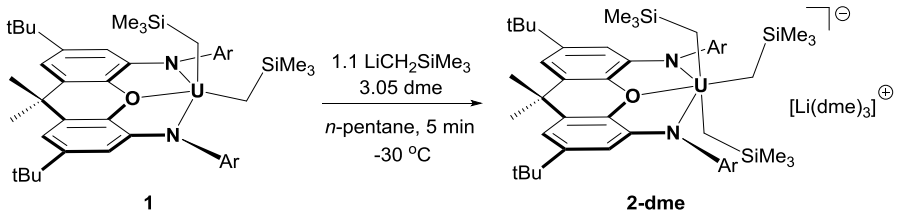

In the solid-state, **2-dme**·2 dme features two independent but structurally similar ion-pairs in the unit cell, each comprised of an XA_2-uranium(IV) trialkyl anion (Figure 2) and a distal $[Li(dme)_3]^+$ cation. Uranium is six-coordinate with the five anionic donors {N(1), N(2), C(48), C(52), and C(56)} in a distorted trigonal-bipyramidal arrangement around the metal centre; the N(1)−U−N(2), N(1)−U−C(48) and N(2)−U−C(48) angles in the equatorial plane are 123.5(3)−124.2(3), 102.2(3)−108.4(3), and 127.4(4)−134.2(3)° respectively, and the C(52)−U−C(56) angle between axial substituents is 159.1(3)−172.8(4)° (τ_{avg} = 0.59 for the two anions in the unit cell) [8]. The neutral diarylether donor is coordinated between the two amido groups, located 0.75 and 0.83 Å out of the N(1)/U/N(2) plane, resulting in a capped trigonal-bipyramidal geometry with an O–U–C(56) angle of 76.5(3) −86.3(3)° and an O–U–C(52) angle of 110.0(3)−110.5(3)°.

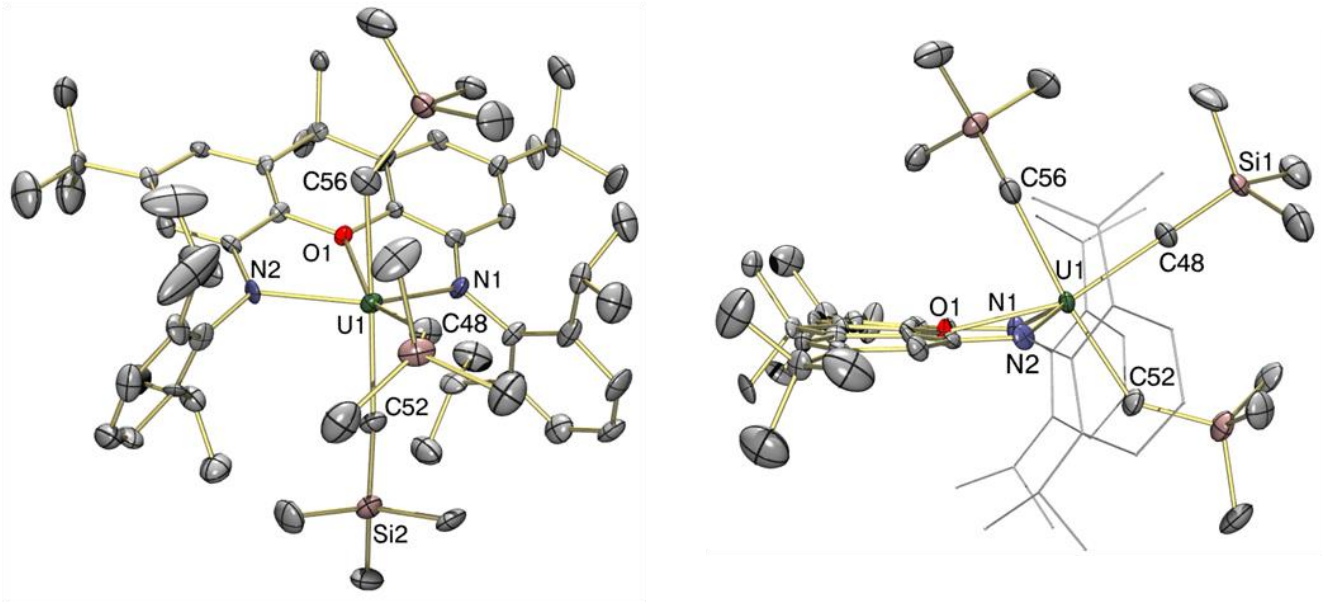

Figure 2. X-ray crystal structure of $[Li(dme)_3][(XA_2)U(CH_2SiMe_3)_3]\cdot 2$ dme (**2-dme**·2 dme), with thermal ellipsoids at 50% probability. Only one of the two independent anions in the unit cell is shown. Hydrogen atoms, the $[Li(dme)_3]^+$ countercation, and dme lattice solvent are omitted for clarity. One *tert*-butyl group is disordered, and only one of the two orientations is shown.

The U–N, U–O, and U–CH_2 distances in **2-dme** are 2.374(9)–2.398(8), 2.515(6)–2.551(6), and 2.42(1)–2.50(1) Å, respectively. The average U−N bond distance in **2-dme** is elongated by 0.12 Å, relative to those of the neutral bis(trimethylsilylmethyl) precursor **1**, likely a result of the increased coordination number, reduced electrophilicity, and steric crowding at the uranium centre. Indeed, uranium–ligand bond elongation has previously been observed in 'ate' derivatives relative to their neutral precursors. For example, Liddle and co-workers observed U=C and U−N_{pincer} bond elongations of at least 0.08 Å in the mixed imido/amido bis(iminophosphorane)methanediide 'ate' derivative $[(BIPM^{TMS})U{=}NCPh_3(NHCPh_3)(K)]$ ($BIPM^{TMS}$ = κ^3-$\{C(PPh_2NSiMe_3)_2\}^{2-}$) relative to those of the neutral bis(amido) precursor $[(BIPM^{TMS})U(NHCPh_3)_2]$ [9]. The U−CH_2 distances in **2-dme** are likely also elongated relative to those in **1**, but the differences fall within the error associated with the measurements; the range of distances observed for **2-dme** does include that observed in Hayton's tris(trimethylsilylmethyl) 'ate' complex $[Li(dme)_3][U(O^tBu)_2(CH_2SiMe_3)_3]$ (U−C = 2.49(1) Å) [10].

Crystallographically-characterized examples of monomeric actinide(IV) tris(alkyl) complexes are surprisingly rare; prominent examples are $[Li(dme)_3][U(O^tBu)_2(CH_2SiMe_3)_3]$ [10], [(BDPP*)Th(μ-Me)$_2$Li(dme)] (BDPP* = $[2,6\text{-}(NC_5H_3)(CH_2NAr)(CH_2N\{C_6H_3{}^iPr(CMe_2)\text{-}2,6\}]^{3-}$; Ar = 2,6-$^iPr_2C_6H_3$) formed by cyclometallation of [(BDPP)ThMe$_3${Li(dme)}] {BDPP = 2,6-bis(2,6-diisopropylanilidomethyl)-pyridine}[11], $[Li(dme)_3][(XA_2)UMe_3]$ [4], and $[Cp^*An(CH_2Ph)_3]$ (An = Th, U) [12, 13] (Figure 3).

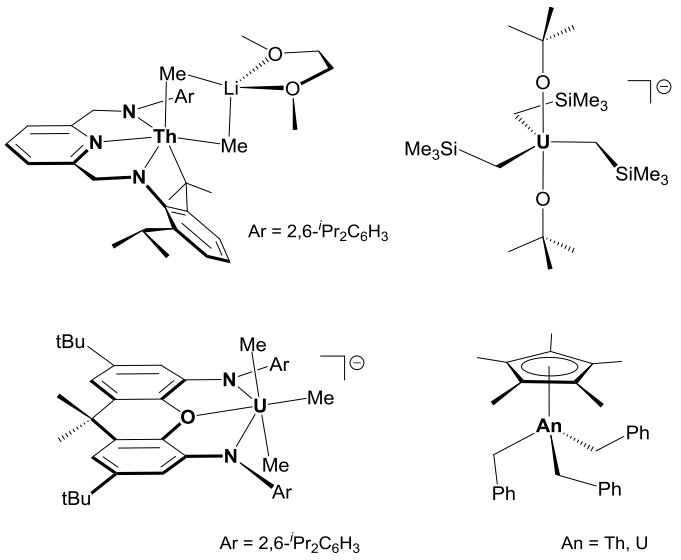

Figure 3. Literature examples of structurally characterized monomeric actinide(IV) tris(alkyl) complexes.

The obtuse U−C−Si angles for the apical alkyl groups in **2-dme** {134.5(6)−140.1(6)°} are comparable to those observed in neutral dialkyl **1**, and are indicative of C−H−U α-agostic interactions. By comparison, the U−C−Si angle for the equatorial alkyl group in **2-dme** {147.9(6)-149.4(6)°} is further expanded, likely due to a combination of C−H−U α-agostic interactions and steric pressure inflicted by the flanking 2,6-diisopropylphenyl groups and neighboring alkyl ligands. A similarly expanded U−C−Si angle {147.5(2)°} was observed for [(^{TIPS2}COT)(Cp*****)U(CH$_2$SiMe$_3$)] (^{TIPS2}COT = {1,4-(Si^{i}Pr$_3$)$_2$C$_8$H$_6$}$^{2-}$), and may in part be a response to the steric pressure afforded by the bulky Si^{i}Pr$_3$ substituents of the cyclooctatetraenide ancillary ligand [14]. The constrained coordination environment

in **2-dme** is also likely responsible for significant N−U−C_{eq} angle-asymmetry; the α-carbon atom of the equatorial CH_2SiMe_3 ligand is shifted towards N(1), resulting in an N(1)−U−C(48) angle of 102.2(3)-108.4(3)°, which is considerably more acute than the complimentary N(2)−U−C(48) angle of 127.4(4)-134.2(3)°.

As mentioned previously, yellow ethereal solutions of **2** in THF or dme decompose at room temperature with release of one equiv of $SiMe_4$. Decomposition of **2** in THF-d_8 afforded a single major product in the ^{1}H NMR spectrum, $[Li(THF\text{-}d_8)_x][(XA_2\text{*})U(CH_2SiMe_3)_2]$ (**3-THF**; XA_2* = [4-(NAr)-5-(N{$C_6H_3{}^i$Pr(CMe$_2$)-2,6})-2,7-^{t}Bu$_2$-9,9-Me$_2$(xanthene)]$^{3-}$; Ar = 2,6-^{i}Pr$_2C_6H_3$); the product of cyclometallation at the methine carbon of an isopropyl group of the XA_2 ligand. This assignment is supported by the presence of 31 paramagnetically-shifted ^{1}H NMR resonances (ranging from +79 to −29 ppm); the full complement of signals expected for C_1-symmetric anion **3** (Supporting Information, Figures S1-S4). Additionally, initial attempts to prepare and crystallize tris(alkyl) 'ate' species **2-dme** afforded both the desired tris(alkyl) complex and pale brown crystals of the cyclometallated derivative $[Li(dme)_3][(XA_2\text{*})U(CH_2SiMe_3)_2]$ (**3-dme**). Complex **3-dme** was also synthesized on a preparative scale by reaction of 1.1 equiv of $LiCH_2SiMe_3$ with dialkyl **1** in neat dme (Scheme 3), followed by stirring the resulting solution of **2-dme** for 1 week at room temperature. After work-up, crude **3-dme** was isolated as a moderately-pure brown powder in 73% yield, but further purification proved challenging, and analytically-pure material was not obtained.

Scheme 3. Cyclometallation of **2-OR$_2$** to yield **3-OR$_2$** (OR_2 = THF or dme; Ar = $C_6H_3{}^i$Pr$_2$-2,6).

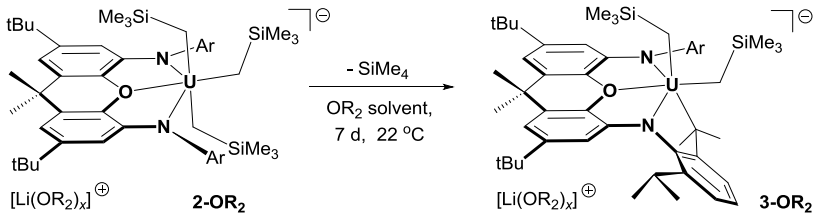

In the solid-state (Figure 4), **3-dme** features a C_1-symmetric XA_2*-uranium(IV) anion and a non-coordinated $[Li(dme)_3]^+$ cation. Uranium adopts a highly distorted six-coordinate geometry, with the two CH_2SiMe_3 groups positioned above and in the plane of the ancillary ligand backbone. The coordinated CMe_2Ar group resides below the N(1)/U/N(2)-plane, forming a five-membered uranacycle incorporating N(1), and as a consequence of cyclometallation, the aryl ring associated with this uranacycle is rotated so as to be less-orthogonal to the xanthene backbone and the N(1)/U/N(2)-plane; the angle between the plane of the aryl ring and the N(1)/U/N(2)-plane is 58° for the cyclometallated 2,6-diisopropylphenyl group and 82° for the intact 2,6-diisopropylphenyl group in anion **3** (cf. the corresponding angles of 76–88° in dialkyl complex **1**). Perhaps to accommodate the strain associated with isopropyl methine cyclometallation, the xanthene backbone of anion **3-dme** is considerably bent; a feature atypical for 6-coordinate XA_2-uranium species {the angle between the two aryl rings of the xanthene backbone is 26.9° in cyclometallated **3-dme** vs. 4.8 and 7.0° in tris(trimethylsilylmethyl) anion **2-dme,** and 6.5° in $[Li(dme)_3][(XA_2)UMe_3]$}.

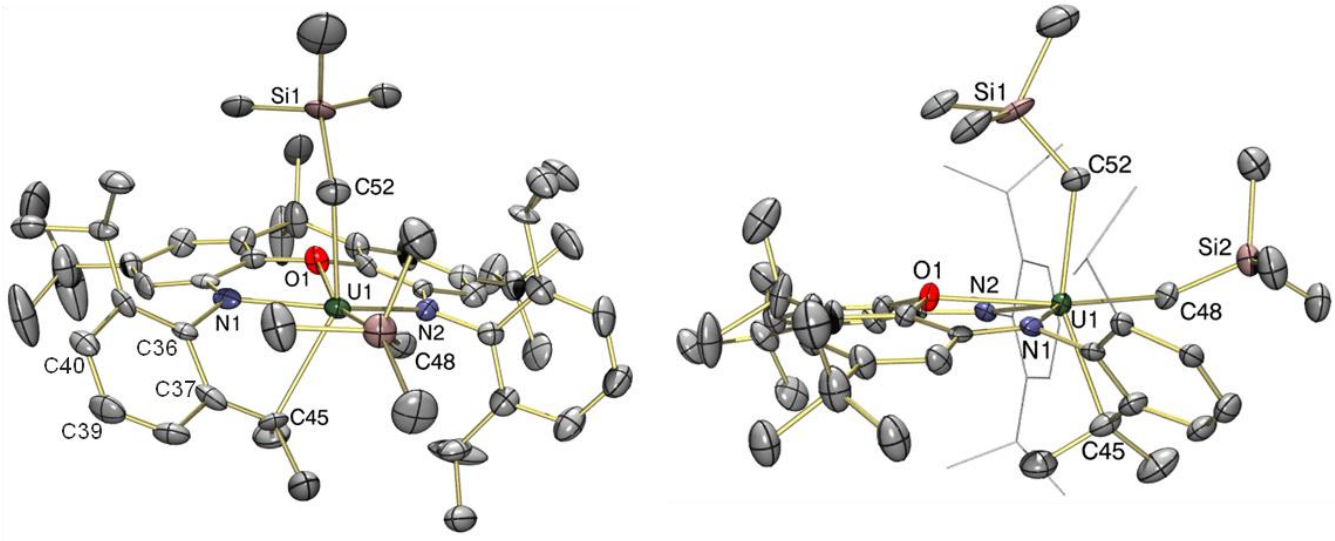

Figure 4. X-ray crystal structure of $[Li(dme)_3][(XA_2*)U(CH_2SiMe_3)_2]$ (**3-dme**), with thermal ellipsoids at 30% probability. Hydrogen atoms and the $[Li(dme)_3]^+$ countercation are omitted for clarity. One *tert*-butyl group is disordered, and only one of the two orientations is shown.

The U−CMe_2Ar bond distance is 2.56(2) Å, whereas the other U−C_{alkyl} bonds in anion **3-dme** are 2.46(2) and 2.47(2) Å. The benzyl-like CMe_2Ar ligand features a relatively acute U−CMe_2−C_{ipso} angle of 97(1)°, likely as a consequence of geometric constraints imposed by the XA_2* ligand. However, it is not possible to rule out some degree of multi-hapto bonding, given the relatively short U−C(36) and U−C(37) contacts (3.05 and 3.10 Å, respectively) and a Cent1–Cent2–U angle of 145.7° {Cent1 = C(39)–C(40) centroid, Cent2 = C(36)–C(37) centroid}. The U−CH_2 and U−N distances in anion **3-dme** are quite comparable to those observed for the tris(trimethylsilylmethyl) precursor **2-dme**, as might be expected given the electronic similarities between the two species.

Cyclometallation of an isopropyl moiety originating from a 2,6-diisopropylphenyl group is fairly common in early transition metal [15] and f-element [16, 17] chemistry, but typically occurs at a *methyl* carbon rather than a *methine* carbon. Rare examples of complexes that engage in isopropyl *methine* metallation include [(BDPP)$ThMe_3${Li(dme)}] [11], [(BDPP)$Lu(AlMe_4)$] [18], [{$CH(CMeNAr)_2$}(X)Ti=CH^tBu] (X = Cl, Br, OTf, BH_4, CH_2SiMe_3; Ar = 2,6-$^iPr_2C_6H_3$) [19, 20], [{$(Me_3Si)_2N$}$_2$Sn=NAr] (Ar = 2,6-$^iPr_2C_6H_3$) [21], [{$CH(CMeNAr)_2$}Me_2Nb=N^tBu] [22], [{$La(AlMe_4)$}$_2$(μ_2-NAr)(μ_3-NAr){(μ_2-Me)$_2$AlMe}] (Ar = 2,6-$^iPr_2C_6H_3$) [23], and [Ar_2Ge=C=C(^{t}Bu)(Ph)] (Ar = 2,4,6-$^iPr_3C_6H_2$) [24].

Reactions of [(XA_2)U(CH_2SiMe_3)$_2$] (1) with Neutral Lewis Bases: Dialkyl complex **1** failed to react with PMe_3, quinuclidine (1-azabicyclo[2.2.2]octane), or 2,2′-bipyridine (bipy) in C_6D_6 between 20 and 40 °C. By contrast, treatment of **1** with one equiv of 4-(dimethylamino)pyridine (DMAP) in C_6D_6 resulted in an immediate colour change from orange to red-orange, and ^{1}H NMR spectroscopy revealed a new collection of extremely broadened and paramagnetically-shifted resonances accompanied by tetramethylsilane. The reaction was repeated on a preparative scale in toluene, and crystallization from *n*-pentane at −30 °C afforded orange crystals of [(XA_2)U(CH_2SiMe_3)(η^2*CN*-

DMAP*)(DMAP)]·2 toluene (**4**·2 toluene; Figure 5); a uranium(IV) monoalkyl complex featuring a neutral κ^1-DMAP ligand and an anionic, η^2*CN*-DMAP* ligand {DMAP* is the anion formed upon deprotonation of DMAP at the 2-position; $NC_5H_3(4\text{-}NMe_2)^-$}. Although one equiv of DMAP was introduced to the reaction, no complex resulting from reaction with only one DMAP ligand was accessible, and reaction of **1** with 2.1 equiv of DMAP in *n*-pentane afforded **4**·*n*-pentane as an analytically-pure bright yellow precipitate in 91% isolated yield (Scheme 4).

Scheme 4. Synthesis of $[(XA_2)U(CH_2SiMe_3)(\eta^2CN\text{-DMAP*})(DMAP)]$ (**4**) (Ar = $C_6H_3{}^iPr_2$-2,6).

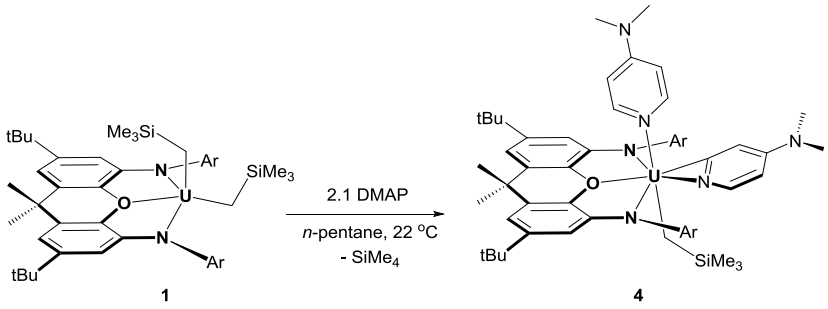

The X-ray crystal structure of **4**·2 toluene (Figure 5) revealed a seven-coordinate C_1-symmetric XA_2-uranium(IV) complex featuring an axially-bound trimethylsilylmethyl ligand, an equatorially-bound η^2*CN*-DMAP* ligand, and an intact κ^1-DMAP ligand coordinated approximately *trans*- to the alkyl substituent. The four anionic donors {N(1), N(2), C(48), and C(52)} and pyridine donor N(3) adopt a distorted trigonal-bipyramidal arrangement around the metal centre, with N(1)−U−N(2), N(1)−U−C(52), and N(2)−U−C(52) angles of 125.41(8), 110.8(1), and 122.1(1)°, respectively, in the equatorial plane, and a C(48)−U−N(3) angle of 169.0(1)° between the axial substituents (τ = 0.73) [8]. The nitrogen donor of the DMAP* ligand, N(6), is located 1.29 Å out of the U/O/N(3)/C(52)/C(48) plane in the direction of N(1), and the neutral diarylether donor is located 0.59 Å out of the N(1)/U/N(2) plane in the direction of the κ^1-DMAP ligand. As typically observed in other XA_2 uranium(IV) species with a coordination number greater than five, the backbone of the XA_2 pincer ligand in **4** is quite planar,

with a 4.9° angle between the xanthene aryl rings {cf. 4.8 and 7.0° in tris(trimethylsilylmethyl) complex **2**, 6.5° in $[Li(dme)_3][(XA_2)UMe_3]$ [4], and 1.2° in $[(XA_2)UCl_2(\mu\text{-}Cl)K(dme)_3]$} [25].

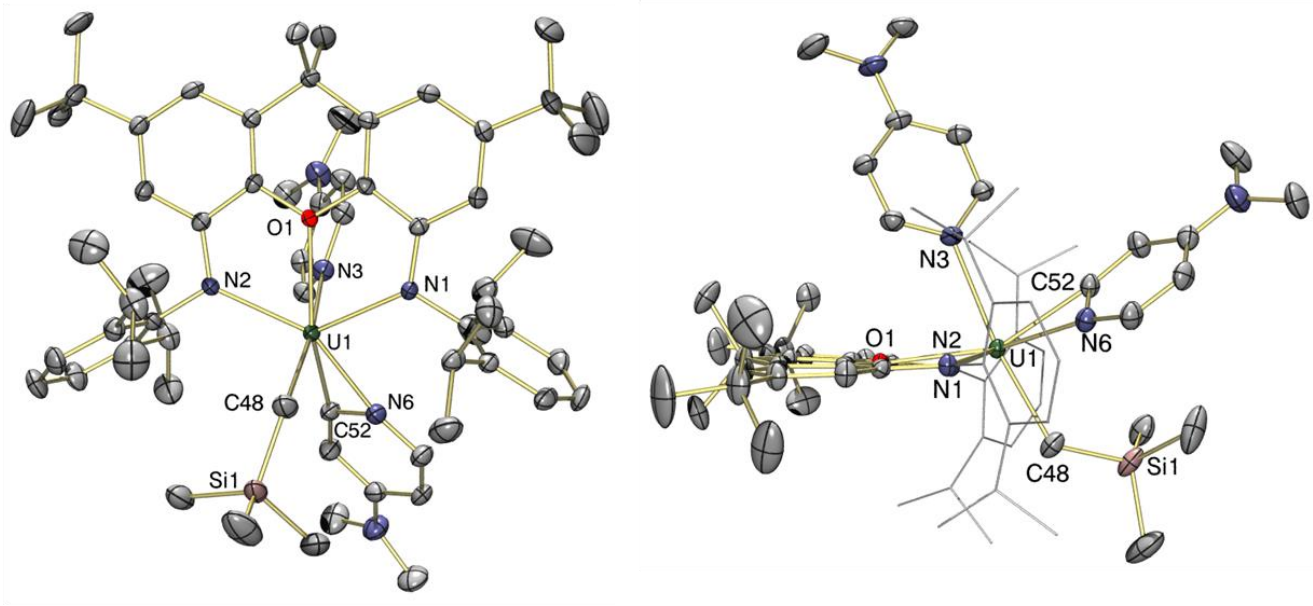

Figure 5. X-ray structure of $[(XA_2)U(CH_2SiMe_3)(\eta^2\textit{CN}\text{-DMAP*})(DMAP)]\cdot 2(toluene)$ (**4**·2(toluene)), with thermal ellipsoids at 50% probability. Hydrogen atoms and two toluene lattice solvent molecules are omitted for clarity.

The U−O, U–N_{pincer}, and U–CH_2 distances in complex **4** are 2.542(2), 2.388(2)–2.395(3), and 2.425(4) Å, respectively, and the U–C–Si angle is 132.1(2)°. These bond lengths are quite comparable to those in sterically-hindered **2**, and the lone U−CH_2 bond distance in **4** does fall within the range observed for certain neutral uranium(IV) trimethylsilylmethyl complexes, including Leznoff's $[(^{DIPP}NCOCN)U(CH_2SiMe_3)_2]$ {$^{DIPP}NCOCN$ = κ^3-$(ArNCH_2CH_2)_2O$; Ar = 2,6-$^i Pr_2C_6H_3$; U–C = 2.40(2)−2.44(2) Å} [26], and Cloke's $[(^{TIPS2}COT)(Cp^*)U(CH_2SiMe_3)]$ ($^{TIPS2}COT$ = {1,4-$(Si^iPr_3)_2C_8H_6$}$^{2-}$; U–C = 2.464(4) Å) [14].

The nitrogen donor of the neutral κ^1-DMAP ligand in complex **4** is coordinated to uranium through a relatively long U−N(3) bond {2.640(3) Å}, which falls at the upper end of the range reported for other uranium(IV) κ^1-DMAP complexes, which are limited to Andersen's $[(Cp')_2U{=}O(DMAP)]$ (Cp' = η^5-$C_5H_2{}^tBu_3$-1,2,4}; U−N = 2.535(4) Å) [27], Liddle's $[(BIPM^{TMS})U{=}NCPh_3(DMAP)_2]$ ($BIPM^{TMS}$ = κ^3-$\{C(PPh_2NSiMe_3)_2\}^{2-}$; $U{-}N_{DMAP}$ = 2.580(5), 2.586(5) Å) [28], and Ding, Walter and Zi's $[Cp^*_2U\{\eta^2$-$C_2(SiMe_3)_2\}(DMAP)]$ (U−N = 2.632(6) Å) [29]. Unsurprisingly, the cyclometallated, anionic η^2*CN*-DMAP* ligand in complex **4** is bound to uranium more intimately than neutral DMAP, with shorter U−N and U−C contacts of 2.367(3) and 2.421(3) Å, respectively, forming a three-membered metallacycle with an acute N(6)−U−C(52) angle of 32.6(1)°.

Uranium-mediated *ortho*-C−H activation of pyridyl derivatives has previously been observed by several groups. Dormond and co-workers originally observed that the four-membered metallacycle $[\{(Me_3Si)_2N\}_2U\{\kappa^2$*CN*-$CH_2SiMe_2NSiMe_3\}]$ cleanly activates an *ortho*-C−H bond of pyridine (and pyridine derivatives), yielding cyclometallated products of the form $[\{(Me_3Si)_2N\}_3U\{\eta^2$*CN*-$(NC_5H_2(4\text{-}R')(6\text{-}R))\}]$ (R = H, R′ = H, Me; R = Me, R′ = H), which were spectroscopically characterized [30]. Scott and co-workers reported that the cyclometallated triamidoamine uranium(IV) complex $[(tren^{TBS*})U]$ ($tren^{TBS*}$ = κ^5-$\{N(CH_2CH_2NR)_2(CH_2CH_2NSi(Me)(^tBu)(CH_2)\}^{4-}$; R = $SiMe_2{}^tBu$) also activates pyridine, forming $[(tren^{TBS})U(\eta^2$*CN*-$NC_5H_4)]$ ($tren^{TBS}$ = κ^4-$\{N(CH_2CH_2NSiMe_2{}^tBu)_3\}^{3-}$; a in Figure 6) with an acute N−U−C angle of 29.2(2)° [31]. Later, Kiplinger and co-workers demonstrated that $[Cp^*_2UMe_2]$ could also activate C−H bonds of pyridine derivatives, yielding similar η^2*CN*-pyridyl products of the form $[Cp^*_2UMe\{\eta^2$*CN*-$NC_5H_2(4\text{-}R')(6\text{-}R)\}]$ (R = H, R′ = H, ^{t}Bu; R = Me, R′ = H; b in Figure 6), with U−N and U−C distances of 2.394(3)−2.424(6) Å and 2.386(3)−2.406(7) Å, respectively, and N−U−C angles ranging from 31.8(3)–32.9(1)° [32, 33]. Additionally, Diaconescu and co-workers reported that $[(^{Fc}NN)U(CH_2Ph)_2]$ (^{Fc}NN = $\{Fc(NSiMe_2{}^tBu)_2\}^{2-}$) reacts with pyridine derivatives to furnish complexes of the form $[(^{Fc}NN)U(CH_2Ph)\{\eta^2$*CN*-$NC_5H_3(6\text{-}R)\}]$ (R = H, Me; c in Figure 6), with U−N and U−C distances of 2.370(4)−2.393(3) Å and 2.397(3)−2.406(5) Å, respectively, and N−U−C

angles of 32.5(1)° [34]. The N(6)−U−C(52) angle {32.6(1)°} and U−N(6) and U−C(52) bond lengths {2.367(3) and 2.421(3) Å} in **4** are in close agreement with those in the aforementioned η^2*CN*-pyridyl complexes of uranium, and while **4** is the first example of a uranium complex featuring a cyclometallated DMAP ligand, C−H activation at the *ortho*-position of DMAP has been observed for thorium [35, 36].

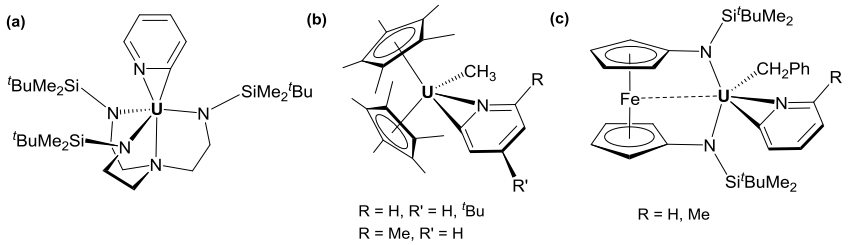

Figure 6. Structurally-characterized uranium complexes featuring η^2*CN*-pyridyl ligands.

The room-temperature ^{1}H NMR spectrum of complex **4** in C_6D_6 or toluene-d_8 is clean but uninformative, featuring 8 extremely broadened resonances between +10 and −10 ppm. The significant broadening of these resonances is likely a consequence of fluxional behaviour involving (a) rotation of the asymmetrically-bound η^2-DMAP* ligand about the U−C(52) bond, and/or (b) neutral DMAP dissociation and re-coordination to yield isomers with different arrangements of the DMAP, DMAP*, and CH_2SiMe_3 ligands within the coordination pocket of the XA_2 ligand. At low-temperature (−70 °C), the ^{1}H NMR spectrum of **4** is indicative of multiple species in solution, but is not completely de-coalesced, so is otherwise difficult to interpret (Supporting Information; Figure S5). However, at high temperature (80–82 °C; Figures S5–S7), the signals coalesce to yield an averaged ^{1}H NMR spectrum featuring 23 paramagnetically shifted resonances between +31 and −72 ppm, indicative of apparent C_s-symmetry. Although **4** can tolerate brief heating at 80 °C, slow decomposition occurs even at 50 °C, yielding $SiMe_4$ and unidentified paramagnetic products.

No intermediates were detected by ^{1}H NMR spectroscopy in the reaction of **1** with DMAP to form **4**. However, this reaction most likely proceeds via initial DMAP coordination to generate [(XA$_2$)U(CH$_2$SiMe$_3$)$_2$(κ^1-DMAP)], followed by σ-bond metathesis to afford HR (R = CH$_2$SiMe$_3$) and [(XA$_2$)U(CH$_2$SiMe$_3$)(η^2*CN*-DMAP*)], and subsequent coordination of the second equivalent of DMAP. This type of direct σ-bond metathesis is common for coordinatively-unsaturated f-element complexes [37]. However, alternative pathways could involve initial σ-bond metathesis to eliminate HR where the H atom originates from (a) an isopropyl group of the XA$_2$ ligand, (b) the γ-position of a CH$_2$SiMe$_3$ ligand, or (c) the α-position of a CH$_2$SiMe$_3$ ligand.

To probe the mechanism by which **4** is formed, the reaction between **1** and DMAP-*d*$_2$ (DMAP deuterated in both *ortho* positions) was monitored *in-situ* by ^{1}H NMR spectroscopy, revealing the formation of Me$_3$SiCH$_2$D as an approximate 2:1 mixture with SiMe$_4$ (Supporting Information; Figure S8). The former product is indicative of direct σ-bond metathesis, while the latter could be due to either adventitious moisture (possibly from incomplete drying of DMAP-*d*$_2$), or a competitive pathway in which the first σ-bond metathesis step does not involve an *ortho*-position of DMAP. Fluxional behaviour prevented conclusive identification of the deuterated isotopomer of the uranium reaction product. However, the uranium product of the reaction with DMAP-*d*$_2$ was isolated in pure form and purposefully decomposed in solution by careful addition of H$_2$O, yielding a ^{2}H NMR resonance attributable to DMAP-*d*$_2$ and/or DMAP-*d*$_1$, with no additional resonances for Me$_3$SiCH$_2$D or deuterium incorporated into the XA$_2$ ligand (Supporting Information; Figure S9), indicative of a single direct σ-bond metathesis pathway as opposed to multiple competing pathways. Kiplinger and co-workers also demonstrated that a direct σ-bond metathesis pathway was responsible for formation of [Cp*****$_2$UMe(η^2*CN*-NC$_5$H$_4$)] via the reaction of [Cp*****$_2$UMe$_2$] with pyridine, since monitoring the reaction with pyridine-*d*$_5$ by ^{1}H NMR spectroscopy revealed the exclusive formation of [Cp*****$_2$UMe(η^2*CN*-NC$_5$D$_4$)] and CH$_3$D [32].

Dialkyl complex **1** was also reacted with 2 equiv of 9-azajulolidine (AJ; a commercially-available, bulky DMAP derivative featuring a fused tricyclic structure), yielding yellow-brown [(XA_2)U(CH_2SiMe_3)(η^2*CN*-AJ*)(AJ)] (**5**) in nearly quantitative yield (Scheme 5). Although 9-azajulolidine has been utilized as a ligand/co-catalyst in copper-catalyzed post-Ullmann C(aryl)−E (E = N, O, S) bond-forming reactions [38], AJ-containing copper species were not described by the authors. Consequently, **5** is the first metal complex of AJ to be identified and crystallographically characterized.

Scheme 5. Preparation of [(XA_2)U(CH_2SiMe_3)(η^2*CN*-AJ*)(AJ)] (**5**) (Ar = $C_6H_3{}^iPr_2$-2,6).

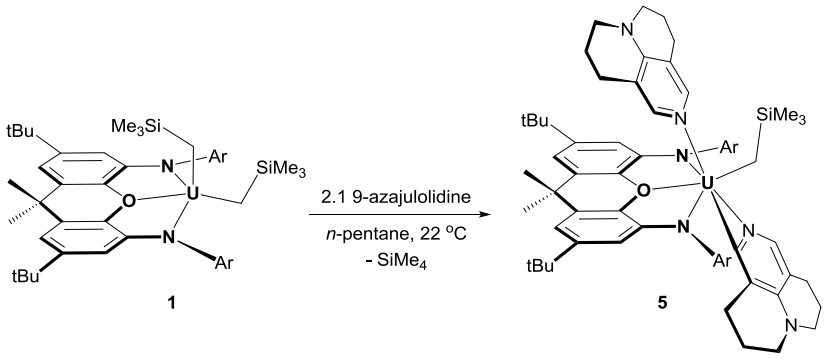

The solid-state structure of **5**·2 *n*-pentane (Figure 7) is similar to that of **4** in that both complexes are seven-coordinate and C_1-symmetric, featuring a lone alkyl group, a cyclometallated η^2*CN*-pyridyl* ligand, and a neutral κ^1-coordinated pyridine ligand. However, in **5**, these ligands are organized differently within the coordination pocket of the XA_2 ancillary; the η^2*CN*-AJ* ligand occupies an axial position, roughly *trans* to the neutral κ^1-AJ donor, and the trimethylsilylmethyl group is bound between the η^2*CN*-AJ* and κ^1-AJ ligands. Additionally, the C(52)–N(3) bond centroid (CN_Cent) lies in the U/O/N(5)/C(48) plane in **5**, whereas C(52) lies in the corresponding plane in **4**.

The amido donors of the XA_2 ligand, N(1) and N(2), the alkyl group, C(48), the pyridine donor, N(5), and CN–Cent adopt a distorted trigonal-bipyramidal arrangement around the metal centre, with

N(1)−U−N(2), N(1)−U−C(48), N(2)−U−C(48) angles of 124.2(2), 113.0(2) and 120.3(2), respectively, in the equatorial plane, and a (CN_Cent)−U−N(5) angle of 168.2° (τ = 0.73) [8]. The neutral diarylether donor is bound relatively far (0.67 Å) above the N(1)/U/N(2)-plane in the direction of the neutral κ^1-AJ ligand. The N(1)/C_{eq}/N(2)-plane of the trigonal-bipyramid in **5** is strongly tilted relative to the plane of the XA_2 donor atoms, more so than in any other XA_2 uranium complex, as indicated by the considerably expanded angle between the N(1)/O/N(2)- and N(1)/C(48)/N(2)-planes of 37.6°. This is likely a consequence of the significant steric pressure asserted by the fused rings of the AJ and AJ* ligands bound to uranium, and is also reflected in O–U–N(5) and O–U–(CN_Cent) angles of 66.5(2) and 125.1°, respectively; short $C_{aryl}\cdots C_{aryl}$ distances of 3.16 and 3.21 Å between aromatic carbon atoms in the AJ ligand and the XA_2 xanthene backbone (those *ortho* to nitrogen and oxygen, respectively) may indicate some degree of π-stacking.

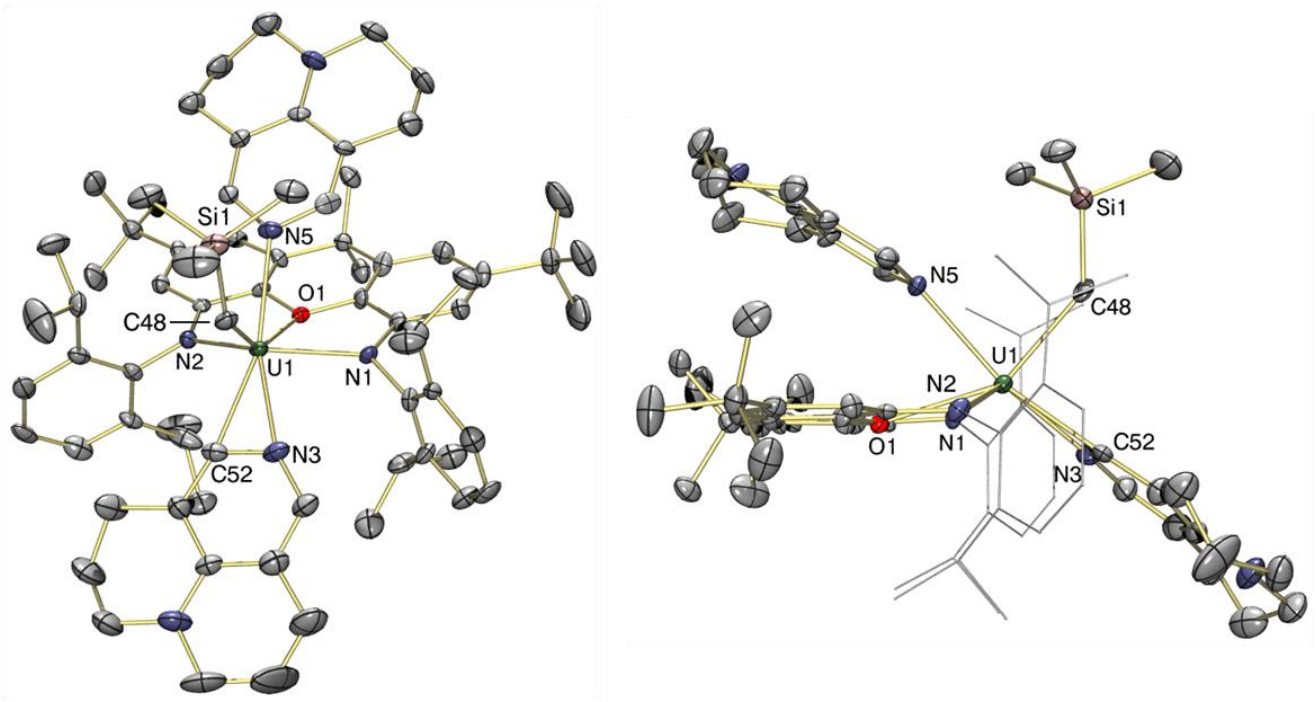

Figure 7. X-ray crystal structure of [(XA_2)U(CH_2SiMe_3)(η^2*CN*-AJ*)(AJ)]·2 *n*-pentane (**5**·2 *n*-pentane), with thermal ellipsoids at 50% probability. Hydrogen atoms and lattice solvent are omitted for clarity. The sp^3 carbon atoms of the AJ* ligand are disordered over two positions, and only one of the two positions is shown.

The U−O (2.557(5) Å), U−N_{pincer} {2.371(6), 2.378(7) Å}, U−C(52) {2.429(8) Å}, and U−$N_{cyclomet.}$ {2.355(7) Å} bond distances, and N(3)−U−C(52) angle {33.1(3)°} in complex **5** are quite comparable to those observed for the related DMAP analogue **4**. However, despite the bulky, fused ring-systems of the AJ substituents, the neutral pyridine group {U−N_{AJ} = 2.579(6) Å} is bound to uranium through a tighter U−N contact in **5** than in **4** {cf. the U−N_{DMAP} distance of 2.640(3) Å in **4**}, likely as a result of the increased donor ability of 9-azajulolidine relative to DMAP [39]. The resulting increased steric hindrance may be responsible for a more obtuse U−C−Si angle of 138.7(4)° in **5** {cf. 132.1(2)° in **4**}.

As with compound **4**, the room-temperature ^{1}H NMR spectrum of **5** in C_6D_6 or toluene-d_8 is clean but uninformative, featuring seven extremely broadened resonances between +8 and −21 ppm. At low-temperature (−81 °C), the ^{1}H NMR spectrum contains > 60 relatively sharp, paramagnetically-shifted resonances (Supporting Information; Figure S10); significantly more than would be expected for any one isomer of complex **5**. This is likely due to isomers of **5** with different relative positions of the alkyl, pyridyl and pyridine ligands, and the solid state structures of **4** and **5**, which differ in exactly this way, lend support to this interpretation. At elevated temperature (60 °C), the ^{1}H NMR resonances of **5** are only marginally coalesced, leading to 14 broad resonances between +11 and −29 ppm (Supporting Information; Figure S11), from which little can be gleaned, and higher temperatures were not accessible due to thermal decomposition of **5**.

Summary and Conclusions

This work highlights the pronounced tendency of 6-coordinate uranium XA_2 alkyl complexes (anionic or neutral) to undergo cyclometallation, in contrast to 5-coordinate neutral dialkyl precursors which are quite thermally robust. Addition of $LiCH_2SiMe_3$ to $[(XA_2)U(CH_2SiMe_3)_2]$ (**1**) formed the tris(alkyl) anion, **2**, and cyclometallation subsequently occurred at an isopropyl methine group of the XA_2 ligand, as previously observed for $[(BDPP)ThMe_3]^-$. By contrast, upon addition of neutral pyridine derivatives

(DMAP and AJ) to **1**, pyridine cyclometallation was observed, followed by coordination of a second equivalent of the neutral donor. These reactions could proceed via various pathways. However, reactions with DMAP-d_2 indicate that a direct σ-bond metathesis pathway is operative in this case.

An intriguing feature of this work is that despite providing dialkyl complex **1** with 2 equiv of either DMAP or AJ, only one pyridine ligand is activated, leaving one remaining alkyl group and one intact pyridine ligand (*cis* to one another in the solid state structure of **5**). Complexes **4** and **5** join five other uranium(IV) η^2*CN*-pyridyl complexes that feature a cyclometallated pyridine ligand and an intact alkyl group (b and c in Figure 6) [32-34], and coordination of a free pyridine ligand certainly appears possible for [Cp*****$_2$UMe(η^2*CN*-NC_5H_4)], given that reaction with excess 2-picoline (2-methylpyridine) yielded [Cp*****$_2$UMe{η^2*CN*-(6-Me(NC_5H_3)}] and liberated pyridine, presumably via undetected [Cp*****$_2$UMe(η^2*CN*-NC_5H_4)(κ^1-2-picoline)] [32].

Experimental Section

General Details. General synthetic procedures have been reported elsewhere [1, 3, 5, 6, 11]. Deuterated solvents were purchased from ACP Chemicals. $LiCH_2SiMe_3$ (1.0 M in *n*-pentane), PMe_3, 2,2′-bipyridine (bipy), quinuclidine (1-azabicyclo[2.2.2]octane), DMAP (4-(dimethylamino)pyridine), 9-azajulolidine, Rh on alumina (5%), and deuterium (99.9 atom%) were purchased from Sigma-Aldrich. Prior to use, solid $LiCH_2SiMe_3$ was obtained by removal of solvent *in vacuo*. DMAP, DMAP-d_2, 9-azajulolidine, quinuclidine, and bipy were sublimed under reduced pressure (<10 mTorr) prior to use, and stored under argon. $H_2[XA_2]$ [3], UCl_4 [13], $[(XA_2)UCl_3\{K(dme)_3\}]$ [25], $[(XA_2)U(CH_2SiMe_3)_2]\cdot$(*n*-pentane) [4], and DMAP-d_2 [40] were prepared using literature procedures.

Combustion elemental analyses were performed on a Carlo Erba EA 1110CHN elemental analyzer at Simon Fraser University by Mr. Farzad Haftbaradaran (with sample preparation conducted by Dr. Wen Zhou of the Leznoff research group at Simon Fraser University). X-ray crystallographic

analyses were performed on suitable crystals coated in Paratone oil and mounted on a SMART APEX II diffractometer with a sealed tube Mo generator with a Triumph monochromator at the McMaster Analytical X-Ray (MAX) Diffraction Facility. Data were collected at 100 K. Two molecules of dme in the unit cell of **2-dme**·2 dme (Z = 8) were highly disordered and could not be modeled satisfactorily and so were treated using the SQUEEZE routine [41]. Complexes **2-dme** and **3-dme** were determined to be inversion twins.

^{1}H and ^{2}H NMR spectroscopy was performed on Bruker DRX-500 and AV-600 spectrometers. All ^{1}H NMR spectra were referenced relative to $SiMe_4$ through a resonance of the employed deuterated solvent or proteo impurity of the solvent: C_6D_6 (δ 7.16 ppm), toluene-d_8 (δ 7.09, 7.01, 6.97, 2.08 ppm), and THF-d_8 (δ 3.58, 1.72 ppm).

All NMR spectra were obtained at room temperature unless otherwise specified. Herein, Aryl = 2,6-diisopropylphenyl, and the numbering scheme ($CH^{1,8}$, $C^{2,7}$, $CH^{3,6}$, $C^{4,5}$, $C^{10/13}$ and $C^{11,12}$) for the xanthene ligand backbone mirrors that used in previous publications [4, 25]. Several peaks in the ^{1}H NMR spectra of paramagnetic uranium(IV) complexes could be assigned on the basis of integration, and in the case of complexes **2-dme** and **4**, the *para* aryl signal appeared as a triplet, allowing definite assignment. The broad resonances integrating to 2H and located at particularly high (>250 ppm) and particularly low (< −70 ppm) frequencies in the spectra of **2-dme** and **4** were speculatively assigned as the UCH_2 protons, given their close proximity to the paramagnetic U(IV) centre. Similarly, the broad resonances integrating to 3H and located at high (>60 ppm) frequency in the spectrum of **3-dme** were assigned as the UCMe_2Ar protons.

[Li(dme)$_3$][(XA$_2$)U(CH$_2$SiMe$_3$)$_3$] (2-dme): A mixture of [(XA$_2$)U(CH$_2$SiMe$_3$)$_2$]·(*n*-pentane) (**1**·*n*-pentane) (0.100 g, 0.087 mmol) and 1.1 equivalents of $LiCH_2SiMe_3$ (0.009 g, 0.095 mmol) were dissolved in minimal *n*-pentane (~ 2 mL) to afford a red solution. The solution was cooled to –30 °C, and 3.05 equivalents of 1,2-dimethoxyethane (dme) were quickly added *via* microsyringe to the rapidly stirring mixture. Immediately upon addition of dme, a yellow precipitate evolved and the supernatant

became a pale orange colour. The mixture continued to stir for ~ 5 minutes and the mother liquors were then discarded, affording a yellow-brown solid. The powder was washed with *n*-pentane (~ 3 mL) and dried, yielding 0.119 g of yellow-brown **2-dme** (0.082 mmol, 95 % yield). X-ray quality crystals of **2-dme**·2 dme were obtained by conducting the reaction in neat dme; the yellow solution was layered with *n*-pentane and cooled to –30 °C. After several days, a mixture of yellow **2-dme**·2 dme crystals were obtained alongside brown crystals of cyclometallated **3-dme**. The ^{1}H NMR spectrum (THF-d_8, 600.1 MHz, 298 K) of **2-dme** is identical to that of the previously reported $[Li(THF\text{-}d_8)_x]^+$ salt [4] except for additional peaks for free dme at 3.42 ppm (12H) and 3.26 ppm (18H). **Anal. Calcd for $C_{71}H_{125}N_2O_7Si_3LiU$:** C, 58.89; H, 8.70; N, 1.93 %. Found: C, 58.99; H, 8.87; N, 2.35%.

$[Li(dme)_3][(XA_2*)U(CH_2SiMe_3)_2]$ (3-dme): Solid $LiCH_2SiMe_3$ (0.009 g, 0.095 mmol, 1.1 equiv) was added to a rapidly stirring solution of $[(XA_2)U(CH_2SiMe_3)_2]$·(*n*-pentane) (**1**·*n*-pentane) (0.100 g, 0.087 mmol) in dme (4 mL) at room temperature. Immediately upon addition, the cherry red solution became yellowy-amber, indicative of $[Li(dme)_3][(XA_2)U(CH_2SiMe_3)_3]$ (**2-dme**) formation *in situ*. Stirring was continued at room temperature for 1 week to complete the cyclometallation reaction, at which point the deep red-brown solution was evaporated to dryness *in vacuo* yielding a deep brown residue. The residue was dissolved in a minimum amount of dme (1 mL) and layered with *n*-pentane. Cooling the mixture at –30 °C for several days resulted in the precipitation of a deep brown oily residue. The residue was washed with *n*-pentane (5 mL), dried *in vacuo*, and finally triturated in *n*-pentane (20 mL) using a sonicating bath. Volatiles were removed *in vacuo* to afford 0.086 g of **3-dme** (0.063 mmol, 73 % yield) as a deep brown powder. Despite numerous attempts, isolated **3-dme** always contained small amounts of unidentified paramagnetic impurities, and as a consequence, a satisfactory elemental analysis could not be obtained for this complex. X-ray quality crystals of **3-dme** were obtained alongside **2-dme**·2 dme after attempted crystallization of **2-dme** from dme/*n*-pentane at –30 °C (*vide supra*). **^{1}H NMR (THF-d_8, 600.1 MHz, 298 K):** δ 78.73, 64.96 (broad s, 2 × 3H, UC*Me*$_2$Ar), 17.65, 5.06, 4.38, 1.32, −4.60, −5.69,

−14.98, −19.35 (broad s, 8 × 3H, C*Me*$_2$, CH*Me*$_2$ {× 3}), 48.11, 45.95, 18.26, 9.42, 8.46, 5.58, 4.17, 2.92, 1.39, −1.56, −2.98, −3.80, −6.66, −9.33, −14.54, −22.93, −28.05 (broad s, 17 × 1H, CH^1, CH^3, CH^6, CH^8, C*H*Me$_2$ {× 3}, Aryl-*meta* CH {× 4}, Aryl-*para* CH {× 2}, UC*H*$_2$ {× 2}), 13.14, 4.04, −6.53, −9.04 (broad s, 4 × 9H, C*Me*$_3$ {× 2}, Si*Me*$_3$ {× 2}), 3.42 (s, 12H, OC*H*$_2$, *free dme*), 3.26 (s, 18H, OC*H*$_3$, *free dme*). **Anal. Calcd for $C_{67}H_{113}N_2O_7Si_2LiU$:** C, 59.18; H, 8.38; N, 2.06 %. Found: C, 56.75–57.65; H, 8.07; N, 2.41–2.64% (two attempts were made)

[(XA$_2$)U(CH$_2$SiMe$_3$)(η^2*CN*-DMAP*)(DMAP)]·*n*-pentane (4·*n*-pentane): Solid DMAP (0.022g, 0.182 mmol) was quickly added to a stirring solution of [(XA$_2$)U(CH$_2$SiMe$_3$)$_2$]·(*n*-pentane) (**1**·*n*-pentane) (0.100 g, 0.087 mmol) in *n*-pentane (3 mL) at room temperature. The red solution stirred for approximately 45 minutes before copious yellow solids precipitated, and stirring was continued for an additional 15 minutes. At this point, 5 mL of *n*-pentane was added, and the mixture was centrifuged. The mother liquors were removed and the bright yellow solids were dried *in vacuo* to yield 0.103 g of **4**·*n*-pentane (0.078 mmol, 91% yield). X-ray quality orange crystals of **4**·2 toluene were grown from toluene/*n*-pentane at –30 °C. Reaction of **1** with 2,6-DMAP-*d*$_2$ followed by identical work-up yielded the *d*$_3$-isotopologue **4-*d*$_3$**·n-pentane. **^{1}H NMR (toluene-*d*$_8$, 500.1 MHz, 298 K):** *δ* 9.81, 7.40 (extremely broad s, 2 × 2H), 8.05 (broad s, 2H), 4.88, −4.08 (v broad s, 2 × 6H), 3.29 {v broad s, 8H (2H + 6H)}, 2.83 {v broad s, 24H (18H (CMe$_3$) + 6H)}, −9.33 (extremely broad s, 9H, SiMe$_3$). **^{1}H NMR (toluene-*d*$_8$, 500.1 MHz, 355 K):** *δ* 30.45, 16.52, −19.19 (broad s, 3 × 1H, DMAP* 3-CH, DMAP* 5-CH, DMAP* 6-CH), 15.43, 14.55, 13.77, 11.14, 7.82, 7.36, 3.19, 1.14 {broad s, 8 × 2H, CH^{1,8}, CH^{3,6}, Aryl-*meta* CH (× 2), C*H*Me$_2$ (× 2), 2,6-DMAP CH, 3,5-DMAP CH}, 10.29 (t, $^3J_{H,H}$ = 8.2 Hz, 2H, Aryl-*para* CH), 5.16, 4.24, 3.82, 3.34, −2.56, −15.12 {broad s, 6 × 6H, CH*Me*$_2$ (× 4), DMAP N*Me*$_2$, DMAP* N*Me*$_2$}, 3.13 (s, 18H, CMe$_3$), −7.25, −9.40 (broad s, 2 × 3H, C*Me*$_2$), −9.06 (broad s, 9H, SiMe$_3$), −71.49 (v broad s, 1 × 2H, UC*H*$_2$). **Anal. Calcd for $C_{70}H_{104}N_6OSiU$:** C, 64.09; H, 7.99; N, 6.41%. Found: C, 64.03; H, 8.13; N, 6.54%.

[(XA$_2$)U(CH$_2$SiMe$_3$)(η^2*CN*-AJ*)(AJ)] (5): Solid 9-azajulolidine (0.032g, 0.182 mmol) was quickly added to a stirring solution of [(XA$_2$)U(CH$_2$SiMe$_3$)$_2$]·(*n*-pentane) (**1**·*n*-pentane) (0.100 g, 0.087 mmol) in *n*-pentane (4 mL) at room temperature. The red-orange solution stirred for 4 hours, at which point the faintly turbid mixture was cooled to –30 °C. After several days, 0.128 g of yellow-brown crystalline solid was harvested and then dried *in vacuo* to provide **5** in 99% yield (0.086 mmol). X-ray quality yellow-brown crystals of **5**·2 *n*-pentane were grown from *n*-pentane at –30 °C. **^{1}H NMR (toluene-*d*$_8$, 600.1 MHz, 303 K):** δ 7.65, 2.04, −6.19, −7.77, −11.06, −20.74 (extremely broad s × 6), −3.14 (v broad s). **^{1}H NMR (toluene-*d*$_8$, 600.1 MHz, 333 K):** δ 10.08, 9.13, 7.52, 5.76, 2.27, −1.24, −6.41, −11.45, −19.27, −28.44 (extremely broad s × 10), 9.04 (s), 4.37, 3.36, −4.90 (v broad s × 3). **Anal. Calcd for C$_{73}$H$_{100}$N$_6$OSiU:** C, 65.25; H, 7.50; N, 6.25%. Found: C, 65.29; H, 7.92; N, 6.40%.

SUPPLEMENTARY DATA

Supplementary Data related to this article (a table of crystallographic bond lengths and angles for **1**-**5** and ^{1}H NMR spectra) can be found at http://dx.doi.org/10.1016/j.jorganchem.xxxxxxxxxxxxx. CCDC 1560254-1560257 contain the supplementary crystallographic data for compounds **2**, **3**, **4** and **5**, respectively.

AUTHOR INFORMATION

Corresponding Author

* Phone: 905-525-9140. Fax: 905-522-2509. E-mail: emslied@mcmaster.ca.
Web: http://www.chemistry.mcmaster.ca/emslie/emslie.html

ACKNOWLEDGMENT

D.J.H.E. thanks NSERC of Canada for a Discovery Grant and N.R.A. thanks the Government of Ontario for an Ontario Graduate Scholarship (OGS) and McMaster University for a Richard Fuller Memorial Scholarship. We are very grateful to Dr. Wen Zhou in the Leznoff group at Simon Fraser University for preparing and submitting Elemental Analysis samples on our behalf.

KEYWORDS

Actinide Complexes / Uranium / Pincer Ligands / Alkyl Complexes / Cyclometallation

REFERENCES

1 C.A. Cruz, T. Chu, D.J.H. Emslie, H.A. Jenkins, L.E. Harrington, J.F. Britten, J. Organomet. Chem. 695 (2010) 2798-2803.

2 K.S.A. Motolko, D.J.H. Emslie, H.A. Jenkins, Organometallics 36 (2017) 1601-1608.

3 C.A. Cruz, D.J.H. Emslie, L.E. Harrington, J.F. Britten, C.M. Robertson, Organometallics 26 (2007) 692-701.

4 N.R. Andreychuk, S. Ilango, B. Vidjayacoumar, D.J.H. Emslie, H.A. Jenkins, Organometallics 32 (2013) 1466-1474.

5 C.A. Cruz, D.J.H. Emslie, L.E. Harrington, J.F. Britten, Organometallics 27 (2008) 15-17.

6 C.A. Cruz, D.J.H. Emslie, C.M. Robertson, L.E. Harrington, H.A. Jenkins, J.F. Britten, Organometallics 28 (2009) 1891-1899.

7 K.S.A. Motolko, D.J.H. Emslie, J.F. Britten, RSC Advances 7 (2017) 27938-27945.

8 The τ parameter is a structural descriptor for 5-coordinate complexes indicating the degree of trigonality; $\tau = (\beta - \alpha)/60$, where β and α are the two greatest bond angles in the complex ($\beta > \alpha$). For a perfectly square-pyramidal geometry, $\tau = 0$; for a perfectly trigonal-bipyramidal geometry, $\tau = 1$. See: A.W. Addison, T.N. Rao, J. Reedijk, J. van Rijn, G.C. Verschoor, J. Chem. Soc. Dalton Trans. (1984) 1349-1356.

9 E. Lu, F. Tuna, W. Lewis, N. Kaltsoyannis, S.T. Liddle, Chem. Eur. J. 22 (2016) 11554-11558.

10 S. Fortier, J.R. Walensky, G. Wu, T.W. Hayton, J. Am. Chem. Soc. 133 (2011) 11732-11743.

11 C.A. Cruz, D.J.H. Emslie, H.A. Jenkins, J.F. Britten, Dalton Trans. 39 (2010) 6626-6628.

12 E.A. Mintz, K.G. Moloy, T.J. Marks, V.W. Day, J. Am. Chem. Soc. 104 (1982) 4692-4695.

13 J.L. Kiplinger, D.E. Morris, B.L. Scott, C.J. Burns, Organometallics 21 (2002) 5978-5982.

14 J.A. Higgins, F.G.N. Cloke, S.M. Roe, Organometallics 32 (2013) 5244-5252.

15 For examples of *early transition metal* complexes featuring activation of an *N*-2,6-$^{i}Pr_2C_6H_3$ group at the isopropyl *methyl* moiety, see: (a) E. Otten, P. Dijkstra, C. Visser, A. Meetsma, B. Hessen, Organometallics 24 (2005) 4374-4386; (b) L.K Knight, W.E. Piers, P. Fleurat-Lessard, M. Parvez, R. McDonald, Organometallics 23 (2004) 2087-2094; (c) F. Basuli, B.C. Bailey, J.C. Huffman, D.J. Mindiola, Organometallics 24 (2005) 3321-3334.

16 For examples of *f-element* complexes featuring activation of a 2,6-$^{i}Pr_2C_6H_3$ group at the isopropyl *methyl* moiety, see: (a) A. Athimoolam, S. Gambarotta, I. Korobkov, Organometallics 24 (2005) 1996-1999; (b) A.C. Behrle, L. Castro, L. Maron, J.R. Walensky, J. Am. Chem. Soc. 137 (2015) 14846-14849.

17 K.R.D. Johnson, P.G. Hayes, Chem. Soc. Rev. 42 (2013) 1947-1960.

18 M. Zimmermann, F. Estler, E. Herdtweck, K.W. Törnroos, R. Anwander, Organometallics 26 (2007) 6029-6041.

19 F. Basuli, B.C. Bailey, L.A. Watson, J. Tomaszewski, J.C. Huffman, D.J. Mindiola, Organometallics 24 (2005) 1886-1906.

20 F. Basuli, B.C. Bailey, J.C. Huffman, D.J. Mindiola, Organometallics 24 (2005) 3321-3334.

21 Ossig, G.; Meller, A.; Freitag, S.; Herbst-lrmer, R. *J. Chem. Soc., Chem. Commun*, **1993**, 497.

22 T.L. Gianetti, R.G. Bergman, J. Arnold, J. Am. Chem. Soc. 135 (2013) 8145-8148.

23 D. Schädle, C. Schädle, D. Schneider, C. Maichle-Mössmer, R. Anwander, Organometallics 34 (2015) 4994-5008.

24 B.E. Eichler, D.R. Powell, R. West, Organometallics 18 (1999) 540-545.

25 B. Vidjayacoumar, S. Ilango, M.J. Ray, T. Chu, K.B. Kolpin, N.R. Andreychuk, C.A. Cruz, D.J.H. Emslie, H.A. Jenkins, J.F. Britten, Dalton Trans. 41 (2012) 8175-8189.

26 K.C. Jantunen, F. Haftbaradaran, M.J. Katz, R.J. Batchelor, G. Schatte, D.B. Leznoff, Dalton Trans. (2005) 3083-3091.

27 G.F. Zi, L. Jia, E.L. Werkema, M.D. Walter, J.P. Gottfriedsen, R.A. Andersen, Organometallics 24 (2005) 4251-4264.

28 E. Lu, O.J. Cooper, F. Tuna, A.J. Wooles, N. Kaltsoyannis, S.T. Liddle, Chem. Eur. J. 22 (2016) 11559-11563.

29 L. Zhang, B. Fang, G. Hou, L. Ai, W. Ding, M.D. Walter, G. Zi, Dalton Trans. 45 (2016) 16441-16452.

30 A. Dormond, A.A. El Bouadili, C. Moise, J. Chem. Soc., Chem. Commun. (1985) 914-916.

31 R. Boaretto, P. Roussel, N.W. Alcock, A.J. Kingsley, I.J. Munslow, C.J. Sanders, P. Scott, J. Organomet. Chem. 591 (1999) 174-184.

32 J.A. Pool, B.L. Scott, J.L. Kiplinger, J. Alloy. Compd. 418 (2006) 178-183.

33 J.L. Kiplinger, B.L. Scott, E.J. Schelter, J. Tournear, J. Alloy. Compd. 444 (2007) 477-482.

34 S. Duhovic, M.J. Monreal, P.L. Diaconescu, Inorg. Chem. 49 (2010) 7165-7169.

35 B. Fang, L. Zhang, G.H. Hou, G.F. Zi, D.C. Fang, M.D. Walter, Chem. Sci. 6 (2015) 4897-4906.

36 C. Zhang, P. Yang, E. Zhou, X. Deng, G. Zi, M.D. Walter, Organometallics (2017), DOI: 10.1021/acs.organomet.7b00212.

37 P.L. Arnold, M.W. McMullon, J. Rieb, F.E. Kühn, Angew. Chem. Int. Ed. 54 (2015) 82-100.

38 K.-T. Wong, S.-Y. Ku, F.-W. Yen, Tetrahedron Lett. 48 (2007) 5051-5054.

39 R. Tandon, T. Unzner, T.A. Nigst, N. De Rycke, P. Mayer, B. Wendt, O.R.P. David, H. Zipse, Chem. Eur. J. 19 (2013) 6435-6442.

40 G.P. McGovern, F. Hung-Low, J.W. Tye, C.A. Bradley, Organometallics 31 (2012) 3865-3879.

41 P.V.D. Sluis, A.L. Spek, Acta Crystallogr. A46 (1990) 194.